RSC Advances

PAPER

Cite this: *RSC Adv.*, 2016, **6**, 64921

Accessing Centnerszwer's quasiracemate – molecular shape controlled molecular recognition†

Jacqueline M. Spaniol and Kraig A. Wheeler*

M. Centnerszwer's seminal 1899 report investigated the stereochemical relationship between optical antipodes of different substances using melting-point behavior. One intriguing melting-point phase diagram produced from this early investigation combined (+)-2-chlorosuccinic acid [(+)-**1**] and (−)-2-bromosuccinic acid [(−)-**2**]. While Centnerszwer's data clearly indicates the formation of a quasiracemic phase – *i.e.*, materials constructed from pairs of isosteric molecules of opposite handedness – at the 1 : 1 component ratio, this material is energetically less favorable than the chiral counterparts. The consequence of this crystal instability is significant as evident by the absence of literature sited crystal structures for the quasiracemic phase (+)-**1**/(−)-**2** and racemates (±)-**1** and (±)-**2**. This study circumvented this challenge by generating multi-molecular assemblies using additional crystallizing agents capable of complementing the hydrogen-bond abilities of succinic acids **1** and **2**. Both imidazole (Im) and 4,4′-bipyridyl-*N*,*N*′-dioxide (BPDO) served as tailor-made additives that effectively modified the crystal packing landscape of quasiracemate of (+)-**1**/(−)-**2**. Combining imidazole with the quasiracemate, racemate, and enantiopure forms of **1** and **2** resulted in crystal structures characterized as molecular salts with layered motifs formed from highly directional N^+–H···carboxylate and carboxyl···carboxylate interactions. In contrast to the enantiopure [(+)-**1**·Im and (−)-**2**·Im] and racemic [(±)-**1**·Im and (±)-**2**·Im] systems, neighboring molecular layers observed in quasiracemate (+)-**1**/(−)-**2**·Im are organized by approximate inversion symmetry. Assessment of the crystal packing efficiency for this series of molecular salts *via* crystal densities and packing coefficients (C_k) indicates imidazole greatly alters the crystal landscape of the system in favor of racemic and quasiracemic crystal packing. A similar desymmetrized crystal environment was also realized for the ternary cocrystalline system of (+)-**1**/(−)-**2**·BPDO where the components organize *via* N^+–O^-···carboxyl contacts. This study underscores the importance of molecular shape to molecular recognition processes and the stabilizing effect of tailor-made additives for creating new crystalline phases of previously inaccessible crystalline materials.

Received 30th March 2016
Accepted 24th June 2016

DOI: 10.1039/c6ra08131b

www.rsc.org/advances

1 Introduction

Quasiracemates (or quasiracemic materials) – compounds constructed from equimolar portions of near enantiomers – pose intriguing technological opportunities to examine the impact of molecular shape to molecular alignment. These materials and the quasiracemic approach to supramolecular assembly continue to attract a broad range of disciplines that seek to probe and exploit molecular recognition profiles. Recent investigations have successfully applied the quasiracemic approach to materials and processes such as those focused on asymmetric assessment,[1,2] synthesis,[3,4] and separation.[5,6] The appeal of these materials stems from their ability to form predictable motifs that mimic the structural patterns observed in their racemic counterparts.[7–9] Crystal structure reports of small molecule racemates reveal a strong preference (>92%) for the components to align with inversion symmetry.[10–12] While this penchant for centrosymmetry also translates to all known quasiracemic structures, quasiracemic assemblies take on rigorously non-centrosymmetric patterns due to the structural features of the two chemically distinct components.

The various definitions of quasiracemic compounds found in the literature are decidedly vague, with each describing a common prerequisite linked to the selection of pairs of chemically different molecules of opposite chirality.[3,13,14] This lack of strict descriptors allows for broad flexibility in the design and selection of quasienantiomer components. Coupled with the organizational control exhibited by quasiracemic materials, it is foreseeable this method could lend itself to developing new materials with improved properties. Though several current science areas have been realized or enhanced by implementing

Department of Chemistry, Eastern Illinois University, 600 Lincoln Avenue, Charleston, Illinois, 61920, USA. E-mail: kawheeler@eiu.edu

† Electronic supplementary information (ESI) available: Crystallographic and hydrogen bond tables for (+)-**1**, (−)-**2**, (+)-**1**·Im, (−)-**2**·Im, (±)-**2**·Im, (+)-**1**/(−)-**2**·Im, and (+)-**1**/(−)-**2**·BPDO. CCDC 1470675–1470681. For ESI and crystallographic data in CIF or other electronic format see DOI: 10.1039/c6ra08131b

the quasiracemate approach,[15,16] topics at the forefront of materials science such as energy storage and delivery, catalytic processes of various kinds, and chemical sensors, could all benefit from applications using quasiracemic materials where the complementary shapes of quasienantiomers direct molecular assembly. Future directions such as these are largely limited only by the requisite needs and creativity of the practitioner.

The rich history of quasiracemic materials likely dates back to 1853 with Pasteur's seminal work on the chirality of tartaric acids.[17] One aspect of this work showed that the deliberate multicomponent crystallization of ammonium (+)-bitartrate and ammonium (−)-bimalate resulted in a crystalline 'combination compound' consisting of a 1 : 1 mixture of the two starting components. Some fifty years after Pasteur's report, studies by Centnerszwer[18] and Timmermans[19] provided additional evidence of quasiracemate formation by examining pairs of succinic acid derivatives. However, unlike Pasteur's assessment of material solubility and optical activity, these studies explored the formation of several quasiracemic phases *via* melting-point phase diagrams. Building on these historic studies, Fredga and co-workers critically assessed the melting-point behavior of hundreds of quasiracemic molecular pairs.[20] This extensive effort demonstrated the importance of molecular chirality and isosteric relationships to the successful construction of these bimolecular systems. Fredga's seminal investigations are largely responsible for the development of the quasiracemic approach that has paved the way for more contemporary reports dedicated to understanding the supramolecular tendencies of quasiracemate components. The literature now contains a sizable database in excess of a hundred quasiracemate crystal structures.[14] Without exception, and regardless of structural framework and functional group, each of these crystallographic reports reveals quasiracemic components aligned in the crystal with near inversion symmetry. Because no clear link exists between the observed approximate centrosymmetric organization and the molecular architectures of these quasiracemate components, this collection of structures implies molecular shape often provides a major contributor to the driving force for quasiracemate formation. Similar observations and arguments have been made for purely racemic materials.[10,21,22]

Over the last several years our interest with materials exhibiting quasiracemic behavior has focused on understanding the role of topological features of small organics to the molecular recognition process.[8,12] In many of these investigations, our strategy centered on acquiring complete sets of crystal structures for each quasiracemic family – *i.e.* structures of the quasiracemate, racemates, and homochiral compounds. This approach compared the racemic and enantiopure structures to the motifs observed in the related quasiracemate. In addition to supporting the notion that quasiracemic materials mimic the centrosymmetric patterns found in the racemic compounds, these investigations also reported strong isostructural relationships for many sets of quasiracemic and racemic families. With many of these examples, the unit cell parameters and crystallographic datasets were nearly indistinguishable. Two such reports pursued the crystallographic examination of Pasteur[23] and Karle's[24] early quasiracemates. Though reinvestigating pivotal science from a previous era offers important historical perspectives, a valuable consequence from such studies is the critical entry point these discoveries offer to new science directions of current interest.

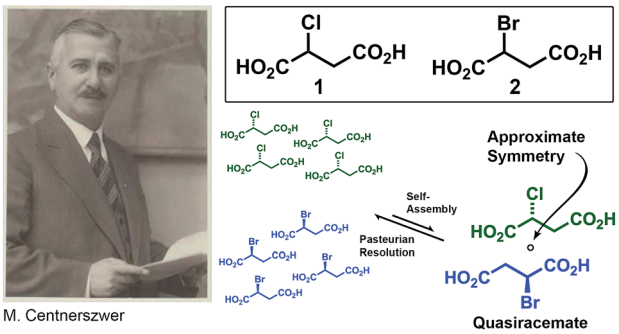

Fig. 1 M. Centnerszwer *circa* 1934 and quasiracemic phase consisting of 2-chloro and 2-bromosuccinic acid (portrait reproduced with permission by Museum Boerhaave, Leiden, Netherlands).

In this study we continue the theme of probing contemporary science from historical perspectives by targeting M. Centnerszwer's 1899 quasiracemate constructed from L-(−)-2-chlorosuccinic acid, (−)-**1**, and D-(+)-2-bromosuccininc acid, (+)-**2** (Fig. 1).[18] While data from Centnerszwer's structurally simple compounds suggest the formation of a new quasiracemate, this material appears less energetically preferred than enantiopure **1** and **2**. This work assesses the viability of isolating crystals of Centnerszwer's quasiracemate and the impact of modifying the packing landscape of this quasiracemate by use of tailor-made additives. Overall, these findings contribute to a growing body of work that examines the fundamental role topological factors play in the molecular recognition process.

2 Experimental section

2.1 Reagents and materials

All chemicals and solvents were purchased from the Aldrich Chemical Co. or Acros Chemicals and used as received without further purification. ^{1}H NMR and ^{13}C NMR spectral data were recorded with a 400 MHz Bruker Ascend spectrometer using TopSpin v.3.2. The spectra were referenced using a solvent residual signal as internal standard. The chemical shift values are expressed as δ values (ppm) and the value of coupling constants (J) in Hertz (Hz). The following abbreviations were used for signal multiplicities: s, singlet; d, doublet; dd, doublet of doublets; t, triplet; q, quartet; m, multiplet; and br, broad.

2.2 Sample preparation

The synthesis of (*S*)-(+)- and (*R*)-(−)-2-chlorosuccininc acid [(+)-**1** and (−)-**1**] was conducted using the following general procedure as previously described.[25] Briefly, a mixture of L-(+)-aspartic acid (10.0271 g, 0.0753 mol) and urea (1.0607 g, 0.0177 mol) dissolved in hydrochloric acid (12 M, 16 mL) and nitric acid (16 M,

16 mL) was heated at 70 °C for 5 hours. The clear-light yellow solution was allowed to stand at room temperature for an additional 18 hours. At that time colorless crystals were filtered and washed with 200 mL of water. The filtrate was neutralized to a pH = 2–3 using a saturated sodium bicarbonate solution and extracted with 3 × 30 mL of ethyl acetate. The organic extracts were combined, dried over anhydrous magnesium sulfate, and reduced under *vacuo* to give (+)-**1** as a colorless solid (4.74 g, 41.4%). Mp 172–174 °C. ^{1}H NMR (acetone-d_6): δ 4.70 (dd, J = 7.46, 6.68 Hz, 1H, H–C_{sp^3}); 3.16 (dd, J = 17.04, 7.46 Hz, 1H, H–C_{sp^3}); 2.95 (dd, J = 17.04, 6.68 Hz, 1H, H–C_{sp^3}). ^{13}C NMR (acetone-d_6): 170.9, 170.0, 52.7, 39.9 ppm.

The synthesis of (*S*)-(+)- and (*R*)-(−)-2-bromosucininc acid [(+)- and (−)-**2**] was achieved *via* the following general procedure as previously described.[26] Briefly, a mixture of D-(−)-aspartic acid (2.0091 g, 0.1509 mol) and potassium bromide (8.2546 g, 0.0699 mol) were dissolved in sulfuric acid (18 M, 39 mL). The vigorously stirred mixture was cooled to −10 °C and a solution consisting of sodium nitrite (1.9978 g, 0.0187 mol) dissolved in 4.10 mL of H_2O was added over a 10 minute period. The clear-brown reaction mixture was then allowed to warm to room temperature and stirred for an additional 5 hours. The crude reaction mixture was then extracted with 3 × 30 mL of ethyl acetate. The organic extracts were combined, dried over anhydrous magnesium sulfate, and reduced under *vacuo* to give (−)-**2** as a colorless solid (2.5075 g, 84.5%). Mp 163–166 °C. ^{1}H NMR (acetone-d_6): δ 4.64 (dd, J = 8.68, 6.16 Hz, 1H, H–C_{sp^3}); 3.25 (dd, J = 17.24, 8.72 Hz, 1H, H–C_{sp^3}); 3.01 (dd, J = 17.24, 6.08, 1H, H–C_{sp^3}). ^{13}C NMR (acetone-d_6): δ 170.3, 169.5, 39.2, 39.0.

2.3 Crystal growth experiments

Crystalline materials prepared for this study were grown in solution using one of two methods. Method A (slow evaporation): the succinic acid or equimolar amounts of imidazole and succinic acid were dissolved in a single solvent or solvent mixture. The solution was left partially covered and allowed to evaporate slowly at −5 °C or room temperature until crystals appeared typically after 2–4 days. Method B (vapour diffusion): equimolar amounts of imidazole and succinic acid were dissolved in a compatible solvent system. A vial containing this solution was then placed in a larger enclosed vessel containing a second precipitating solvent (solvent B) in which the components were insoluble. Crystal growth *via* this method at −5 °C or room temperature typically occurred after 1–3 days.

***S*-(−)- and *R*-(+)-2-chlorosuccinic acid, (−)- and (+)-1.** Colorless plates; method A; room temperature (acetone); mp 172–174 °C.

***S*-(−)- and *R*-(+)-2-bromosuccinic acid, (+)-2.** Colorless plates; method A; room temperature (acetone); mp 161–163 °C.

Imidazolium hydrogen *R*-(+)-2-chlorosuccinate, (+)-1·Im. Colorless prisms; method A; room temperature (1-propanol); mp 125–128 °C.

Imidazolium hydrogen *S*-(−)-2-bromosuccinate, (−)-2·Im. Colorless prisms; method A; −5 °C (1-propanol); mp 121–123 °C.

Imidazolium hydrogen (±)-2-bromosuccinate, (±)-2. Colorless prisms; method B; −5 °C (5 : 1 methanol : water/acetone); mp 130–133 °C.

Imidazolium hydrogen *R*-(+)-2-chlorosuccinate/imidazolium hydrogen *S*-(−)-2-bromosuccinate, (+)-1/(−)-2·Im. Colorless prisms; method A; −5 °C (methanol); mp 125–127 °C. Colorless prisms; method A; −5 °C (1 : 1 methanol : ethanol); mp 125–127 °C. Colorless prisms; method B; −5 °C (1 : 1 methanol : acetone); mp 125–127 °C. Colorless prisms; method B; −5 °C (1 : 1 methanol : ethanol/acetone); mp 125–127 °C.

4,4′-Bipyridine-*N*,*N*′-dioxide *R*-(+)-2-chlorosuccinic acid/*S*-(−)-2-bromosuccinic acid, (+)-1/(−)-2·BPDO. Colorless prisms; method A; −5 °C (methanol); mp 183–185 °C. Colorless plates, method B; −5 °C (methanol/acetone); mp 183–185 °C.

2.4 Characterization

X-ray Crystallography. Crystallographic details for compounds (+)-**1**, (−)-**2**, (+)-**1**·Im, (−)-**2**·Im, (±)-**2**·Im, (+)-**1**/(−)-**2**·Im, (+)-**1**/(−)-**2**·BPDO are summarized in Table S2 (ESI†). X-ray data were collected on a Bruker APEX II diffractometer (Cu-Kα λ = 1.54178 Å; graphite monochromator, T = 100(2) K). Data sets were corrected for Lorentz and polarization effects as well as absorption – SADABS/multi-scan.[27] The criterion for observed reflections is $I > 2\sigma(I)$. Lattice parameters were determined from least-squares analysis and reflection data. Structures were solved by direct methods and refined by full-matrix least-squares analysis on F^2 using X-SEED[28] equipped with SHELX-2014/7.[29] All non-hydrogen atoms were refined anisotropically by full-matrix least-squares on F^2 by the use of the SHELXL[29] program. In the case of disordered (+)-**1**/(−)-**2**·BPDO, the fragment occupancies were refined and constrained to sum 1.0. H atoms for OH and NH groups were located in difference Fourier synthesis and refined isotropically with restrained O–H and N–H distances of 0.85(2) Å and $U_{iso} = 1.2U_{eq}$ of the attached O and N atom. The remaining H atoms were included in idealized geometric positions with $U_{iso} = 1.2U_{eq}$ of the atom to which they were attached. Where appropriate, molecular configurations were compared to the known chirality of the 2-halosuccinic acid components and estimated Flack parameters.[30] Atomic coordinates were inverted to achieve correct molecular configurations where needed.

3 Results and discussion

3.1 Centnerszwer's quasiracemate

M. Centnerszwer's quasiracemate provides a structurally simple system with components that differ by Cl and Br substituents. Given the resources available at the end of the 19th century, it is not surprising this early investigation pursued the effects of co crystallization *via* melting-point data. This method involved generating a series of solid mixtures that differed incrementally by the ratio of components. Collecting melting-point data for each sample then provided a useful tool to probe the thermal properties of these materials. Fig. 2 shows several multi-component phase diagrams consisting of various combinations of 2-chlorosuccinic acid (**1**) and 2-bromosuccinic acid (**2**).

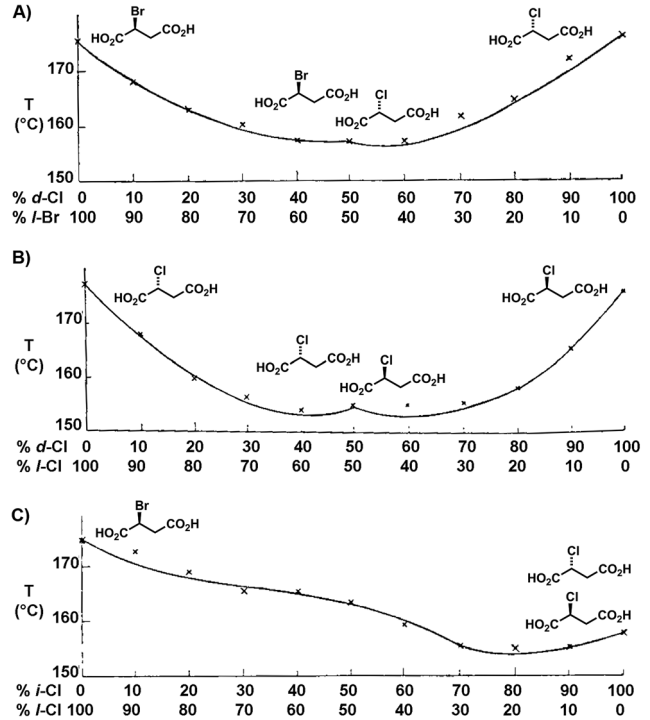

Fig. 2 Centnerszwer's melting-point phase diagrams[18] showing (A) the quasiracemate of (+)-**1** and (−)-**2**, (B) racemate (±)-**1**, and (C) a mixture of (−)-**2** and (±)-**1**.

The melting-point data from Centnerszwer's materials provides an intriguing example that supports the presence of quasiracemate (+)-**1**/(−)-**2** (Fig. 2A). The diagram reveals two eutectic points at component ratios of ~40 : 60 and 60 : 40 with the appearance of quasiracemic phase nearly 20 degrees lower than the homochiral counterparts. A similar melting-point landscape was also recorded for (±)-**1** (Fig. 2B). The melting-point behavior of the ternary system (±)-**1**/(−)-**2** shows the effect of introducing (−)-**1** to the quasiracemic system. The result is an ill-defined diagram complicated by the assortment of interactions arising from this three-component system (Fig. 2C).

The substantially lower melting points associated with the quasiracemic and racemic systems occur infrequently in the literature and likely originates from the differences in packing forces that exist in the crystal lattice. Unlike the melting-point behavior of the majority of racemic compounds, racemates of the type shown in Fig. 2B melt at similar temperatures to that of the 1 : 1 conglomerates. The thermodynamic consequence of this observation on the recognition process is significant. Recrystallization of racemates of this class typically result in mechanical separation *via* a Pasteurian-type resolution process to give distinctly different crystals containing either the (+) or (−) antipodes. Because quasiracemates are close structural relatives to racemic compounds, it is not surprising spontaneous resolution has also been reported for these materials.[31] Two lines of evidence suggest crystal growth of the quasiracemic system consisting of **1** and **2** also undergoes separation. First, Centnerszwer's melting point diagrams indicate racemic and quasiracemic phases with melting points significantly less than the enantiopure compounds. Second, the Cambridge Structural Database (CSD)[32] reports the crystal structures of (−)-**1** (ref. 33) and (+)-**2**,[34] but those corresponding to the racemic forms are suspiciously absent.

Our investigation began with the asymmetric synthesis of **1** and **2** using previously reported procedures.[25,26] These synthetic transformations involved diazotization of either D- or L-aspartic acid with $NaNO_2$/HX. This approach followed the *in situ* preparation of diazonium intermediates that underwent further double substitution reactions to give the desired 2-halosuccinic acids with retained stereochemistry as compared to the starting aspartic acid.

Attempts to grow crystals of Centnerszwer's quasiracemate involved combining equimolar portions of (+)-**1** and (−)-**2**. Crystal growth experiments using this mixture ranged from standard solution techniques employing a variety of solvents to crystal growth from the melt. Materials retrieved from these studies consisted of either the starting homochiral Cl- or Br-succinic acids or amorphous conglomerate solids as determined by melting point or X-ray diffraction data. Previously examined room-temperature crystal structures of (−)-**1** (ref. 33) and (+)-**2** (ref. 34) were re-determined at 100 K for this study. Crystallographic assessment of these materials are isostructural with closely related unit cell parameters and crystal alignment. These structures consist of molecules linked by $R_2^2(8)$ carboxyl···carboxyl contacts to give chain motifs propagating along the *a*-axis (Fig. 3A). Adjacent inversion related motifs to these chains organize with effective close-packing as compared to other small organic carboxylic acids (Fig. 3B).[35] The crystal densities [(−)-**1**, 1.740 g mL^{-1}; (+)-**2**, 2.168 g mL^{-1}] and packing coefficients (C_k, a measure of free space in crystals (ref. 36 and 37)) [(−)-**1**, 81.6%; (−)-**2**, 81.7%] suggest relatively high packing

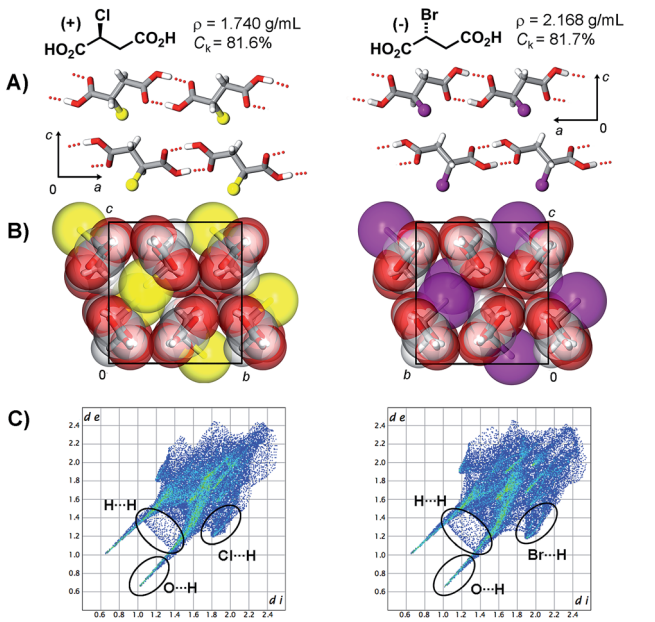

Fig. 3 Crystal structure projections of isostructural (−)-**1** and (+)-**2** depicting (A) $R_2^2(8)$ carboxyl···carboxyl motifs, (B) close-packing of unit cell, and (C) fingerprint plots.

efficiency. Perhaps another indication of the compact alignment of these materials comes from comparison to the crystal densities of the structurally related achiral 2-chloro and 2-bromofumaric acids.[38,39] While it is foreseeable these species could adopt planar geometries that translate to efficient crystal stacking, their densities are markedly less (Cl, 1.66 g mL^{-1}; Br, 2.07 g mL^{-1}) than (−)-**1** and (+)-**2**. We reasoned that our unsuccessful attempts to prepare crystals of quasiracemate **1**/**2**, combined with the packing efficiency of (−)-**1** and (+)-**2**, offers further support that the thermodynamic stability of these enantiomers components outweighs the benefit of crystallizing the racemic or quasiracemic mixtures.

3.2 Multi-molecular assemblies of Centnerszwer's quasiracemate

Moving forward, our attention then turned to pursuing Centnerszwer's quasiracemate by creating multi-molecular assemblies of **1** and **2** with the aid of the cocrystallization method. This strategy exploits the complementary structural features and non-bonded contacts between chemically distinct components. The successful use of tailor-made additives to engender desired chemical functions on multi-molecular systems has experienced considerable attention in the literature.[40,41] The motivation for applying this approach to the current study rests with the opportunity to create new crystalline phases with different thermodynamic properties to that of the starting components. Since the molecular framework for succinic acids **1** and **2** consists of a pair of carboxyl groups, it was initially important to consider secondary molecules that take advantage of the hydrogen-bond ability of one or both CO_2H groups. The non-bonded behavior of carboxylic acids in the presence of a variety of functional groups is well documented.[42] Because these reports provide a substantial list of secondary molecules that create persistent assemblies with carboxylic acids, a potential obstacle facing this study focused on narrowing the possible selection of components to be paired with succinic acids **1** and **2**. A search of the CSD for entries containing multi-component systems with either **1** or **2** offered valuable insight to the crystallization preferences of these succinic acids. One critical entry, the structure of imidazolium (±)-2-chlorosuccinate by MacDonald *et al.*, gave direct support to the accessibility of a racemic crystalline phase involving component **1** and imidazole.[43]

With the aid of this structural information, the investigation then turned to preparing a series of compounds that contain imidazole (Im) and succinic acids **1** and **2**. To understand the supramolecular preferences of combining these components, this study included not only the quasiracemate (−)-**1**/(+)-**2**·Im, but also the structures of the racemic and enantiopure compounds – 5 crystal structures total. The asymmetric units and crystal packing views of this family of structures are provided in Fig. 4A–E. Crystal growth experiments of these multi-molecular systems utilized both slow evaporation and vapor diffusion techniques. An unanticipated outcome was the discovery crystallization of (±)-**2** or (−)-**2** with imidazole under ambient conditions gave crystals of the substitution product 3-carboxy-2-(imidazol-3-ium-1-yl)propanoate.[44–47] To avoid this unwanted transformation and to promote crystal growth of the desired multi-molecular compounds, all crystallization studies involving bromo **2** in the presence of imidazole were conducted at −5 °C. Crystalline samples retrieved from this study were initially examined by melting point (mp) determinations. Unlike Centnerszwer's report of the mp trend for the family of succinic acids **1** and **2** [*i.e.*, (+)-**1**, (−)-**2**, (±)-**1**, and (+)-**1**/(−)-**2**; Fig. 2], the effect of combining imidazole with these succinic acids sufficiently alters the crystalline landscapes to promote crystal growth of the racemic materials. The mp values for molecular salts (+)-**1**·Im and (−)-**2**·Im are 125–128 °C and 121–123 °C, respectively. By contrast, those mp values for (±)-**1**·Im (134–137 °C, ref. 43) and (±)-**2**·Im (130–133 °C) are higher suggesting the homochiral imidazolium salts take on destabilized crystalline phases compared to their racemic counterparts. In turn, the consequence of this thermal property trend is that it poses a potential scenario for the formation of quasiracemate (+)-**1**/(−)-**2** involving imidazole as an additional crystallizing agent.

Inspection of the crystal structures generated for this series of compounds reveals several noticeable similarities with the molecular and supramolecular structures. In each case, the asymmetric units consists of a molecular salt derived from monohydrogen succinate and imidazolium components. These ions link *via* N^+–H···carboxylate interactions with $N^+\cdots O^-$ and $H\cdots O^-$ bond lengths ranging from 2.67–2.74 Å and 1.87–1.94 Å, respectively, with average distances of 2.72 and 1.90 Å. The nature of these interactions is quite directional as evident from an average N–H···O angle of 167° (154 to 177°). These motifs link with translationally related neighbors to give molecular chains.

A second distinct interaction involves the succinate component participating in carboxyl···carboxylate contacts. The role of the O–H···$^-$O interaction to crystal stabilization is significant with short hydrogen-bond contacts [O···$^-$O, 2.54 and 2.60 Å (2.57 Å (average)); H···$^-$O, 1.69–1.77 Å (1.73 Å (average)) and nearly linear O–H···$^-$O angles [170–176° (173° (average))]. This supramolecular synthon connects adjacent monohydrogen succinate entities to form molecular chains. Because the two primary hydrogen-bond contacts (*i.e.*, carboxylate···imidazolium and carboxyl···carboxylate) observed for this family of imidazolium salts propagate in orthogonal directions, the result is the construction of robust molecular layers. This 2D motif provides a common feature inherent to these structures with variations due to the orientation of neighboring layers.

Quasiracemic crystals for this investigation were prepared by low temperature slow evaporation of a 1 : 1 : 2 mixture of the (+)-**1**, (−)-**2**, and imidazole components. Crystallographic assessment of a crystal retrieved from these experiments indicated molecules organized in non-centrosymmetric space group *P*1 with X-ray reflection data and unit cell parameters nearly indistinguishable to those observed for the racemic structures (space group $P\bar{1}$). Unlike the homochiral (Fig. 4A and E) and racemic (Fig. 4B and D) materials, the asymmetric unit of the quasiracemate consists of a ternary system with components (+)-**1** and (−)-**2** aligned with near inversion symmetry due to

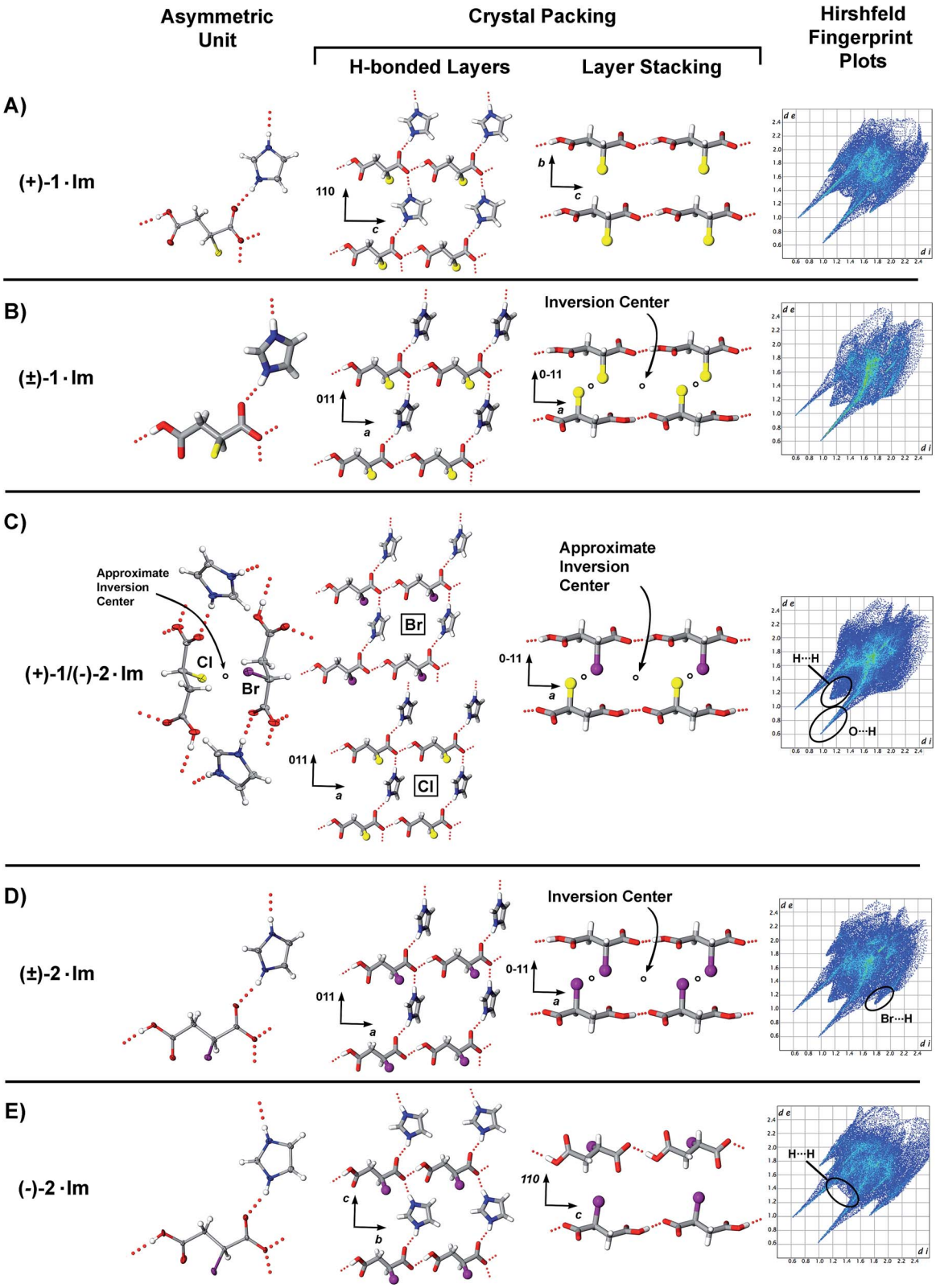

Fig. 4 Crystal structure projections and fingerprint plots for (A) (+)-**1**·Im, (B) (±)-**1**·Im,[43] (C) (+)-**1**/(−)-**2**·Im, (D) (±)-**2**·Im, and (E) (−)-**2**·Im. Except for (±)-**1**·Im, the asymmetric units are depicted with atomic displacement parameters at the 50% level.

complementary molecular shapes of the succinic acid adducts. As shown in Fig. 4B–D, the crystal packing motifs for quasiracemate (+)-**1**/(−)-**2**·Im imitate those observed for racemates (±)-**1**·Im and (±)-**2**·Im. In each structure, the hydrogen-bonded layers align in the (011) plane. For the quasiracemic phase, these molecular layers alternate with motifs constructed from

(+)-**1**·Im and (−)-**2**·Im arrays. The observed translational non-crystallographic symmetry existing between the layers of the quasiracemic phase is the direct result of pairing the quasienantiomeric forms of **1** and **2**. As with all known quasiracemic crystal structures, the assembly of (+)-**1** and (−)-**2** combined with imidazole is predisposed to adopt near inversion symmetry with a high degree of structural mimicry to the local and global crystal packing features of the 'true' racemic compounds.

In contrast to the racemic and quasiracemic phases, the crystal structures of homochiral (+)-**1**·Im and (−)-**2**·Im display significantly different crystal packing with components organized in space groups $P1$ and $P2_1$, respectively (Fig. 4A and E). The structural implication of the imposed space group symmetry is that neighboring hydrogen-bonded layers are either related by translational symmetry or by a two-fold screw axis. As such, the overall patterns from these structures are distinctly non-centrosymmetric.

Evaluating the packing efficiency of this series for structures provided further evidence of the driving force for quasiracemate formation. This was accomplished by comparison of the crystal densities (ρ) and packing coefficients (C_k). These related identifiers of crystal compactness follow a similar trend for this structural family. The crystal structures corresponding to racemates (±)-**1**·Im ($\rho = 1.572$ g mL^{-1}, $C_k = 81\%$) and (±)-**2**·Im ($\rho = 1.883$ g mL^{-1}, $C_k = 83\%$) are appreciably closer packed than those of enantiomers (+)-**1**·Im ($\rho = 1.552$ g mL^{-1}, $C_k = 80\%$) and (−)-**2**·Im ($\rho = 1.801$ g mL^{-1}, $C_k = 80\%$). These trends are consistent with Wallach's Rule[48] and the companion study by Brock *et al.*,[49] where comparison of sets of racemic/chiral pairs indicated racemic crystals are, on average, about 1% more tightly packed than the their chiral counterparts. Our quasiracemate also benefits from the propensity of racemic crystals to align with greater density. Because the crystal structure of (+)-**1**/(−)-**2**·Im is isostructural with racemates (±)-**1**·Im and (±)-**2**·Im, it is not surprising the crystal density ($\rho = 1.572$ g mL^{-1}) and C_k (81%) values reside between those for the racemates. This information surmises that tighter crystal packing of the racemic and quasiracemic systems reflects greater thermodynamic stability. Such a structural bias is significant and suggests packing of the imidazolium succinate racemates or quasiracemate outweighs the potential mechanical separation of components as in the case of the bimolecular (±)-**1**, (±)-**2**, or (+)-**1**/(−)-**2** systems.

3.3 Bipyridine-*N*,*N*′-dioxide quasiracemate

Considering the success of the ternary quasiracemate (+)-**1**/(−)-**2**·Im, we wondered if this study could be further developed by substituting imidazole for other additives. Given the initial design strategy of adopting co-former molecules that complement the hydrogen-bond abilities of succinic acids **1** and **2**, 4,4′-bipyridyl-*N*,*N*′-dioxide (BPDO) seemed a viable candidate for creating a second ternary system with quasiracemate (+)-**1**/(−)-**2**. Many cocrystallization investigations have demonstrated the merit of BPDO as a reliable ditopic hydrogen-bond acceptor.[50] Building on these previous reports, we anticipated molecular architectures constructed from BPDO and succinic acids **1** or **2** to be controlled by N^+–$O^-\cdots$H–O interactions. Fig. 5 shows the outcome from cocrystallizing (+)-**1**, (−)-**2**, and BPDO in a 1 : 1 : 2 ratio. Crystallographic assessment of samples from this experiment revealed that the BPDO and succinic acid components link by the anticipated N^+–$O^-\cdots$carboxyl contacts in space group $P1$. This non-bonded interaction creates molecular chains with alternating BPDO and (+)-**1** or (−)-**2** motifs propagating along the [011] axis. These assemblies further align in the crystal with neighboring (+)-**1**·BPDO and (−)-**2**·BPDO motifs related by approximate inversion symmetry. This desymmetrized arrangement closely mimics the centrosymmetric space group $P\bar{1}$ where the deviation from true symmetry arises from the chemical variation of the Cl and Br groups.

Though the crystal structures of the ternary quasiracemates (+)-**1**/(−)-**2**·Im and (+)-**1**/(−)-**2**·BPDO are markedly different, both take advantage of the complementary structural features of molecular shape and strong hydrogen-bond interactions. The structural consequence of these design elements is the construction of robust molecular assemblies that closely imitate inversion symmetry.

3.4 Hirshfeld surface analysis

The Hirshfeld surface model for assessing atomic interactions in crystals came about in the late 1970's.[51] By partitioning the electron density of atomic fragments in a molecule, this method effectively generates weighted functions for mapping atomic surfaces that are highly sensitive to the immediate crystal environment. Because the Hirshfeld surface is defined by the molecule and the proximity of its nearest neighbours, the generated surface can effectively relay information about the crystal environment and individual intermolecular interactions. This method is sensitive to seemingly small crystal anomalies and thus offers an important structural tool for comparing families of related structures.

A particularly useful application of the Hirshfeld surface has been incorporated into M. A. Spackman's software platform *Crystal Explorer*.[52,53] In addition to offering a practical means to graphically access 3D Hirshfeld surfaces from input molecules, this package also contains a wide-array of structural tools for assessing the properties associated with crystalline assemblies. One such tool targets the parameters d_i and d_e – defined as the

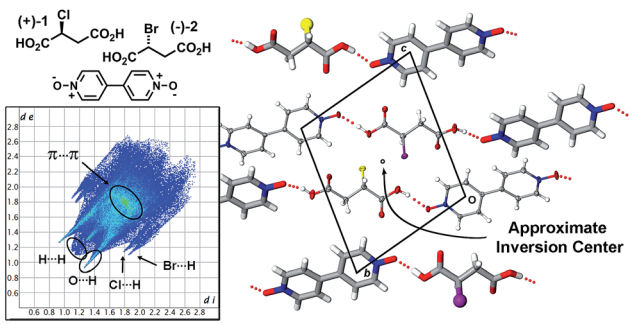

Fig. 5 Crystal structure packing diagram (atomic displacement parameters, 50%) and fingerprint plot for quasiracemate (+)-**1**/(−)-**2**·BPDO.

distance from the Hirshfeld surface to an internal (d_i) and external (d_e) nuclei. By plotting d_i *versus* d_e the result is an informative fingerprint diagram with features highly sensitive to the immediate environment of the molecule.

Applying this method to the current study offers important insight to the structural similarities and variations of this family of succinic acids. For isostructural succinic acids (+)-**1** and (−)-**2**, the fingerprint plots are nearly indistinguishable (Fig. 3C). A dominant contact is depicted as sharp spikes located at the bottom left of the diagrams and signifies an O···H interaction. This combined with the diffuse region (indicating H···H contacts) located between the spikes represents the cyclic $R_2^2(8)$ carboxyl···carboxyl interactions. A second principal contact recognized in Fig. 3 is the Cl/Br···H interaction as identified as a pair spikes with greater separation and at much larger values of d_i and d_e. Unlike the plot features corresponding to the carboxylic acid dimer, these spikes are less pronounced due to the ill-defined nature of these interactions. Visually comparing these plots to those depicted in Fig. 4 for the imidazole molecular salts highlights the common features of strong directional O···H interactions. In the case of the five structures shown in Fig. 4, each lack the diffuse patterns between the pair of O···H spikes. This feature is consistent with sets of acyclic carboxylate···carboxyl contacts present in these structures. The topology represented in the fingerprint plots corresponding to (±)-**1**·Im, (±)-**2**·Im, and quasiracemate (+)-**1**/(−)-**2**·Im are decidedly similar owing to the isostructurality of these racemic and quasiracemic phases. One area of variation in the fingerprint diagrams relates to the Cl/Br···H interactions. While this contact is present in each structure, it is more pronounced in (±)-**2**·Im (Fig. 4D). This same variation is seen with the homochiral (+)-**1**·Im and (−)-**2**·Im structures. The overall differences observed with the patterns in the plots for these homochiral structures are even more distinct and result from the variation in space groups and stacking of molecular sheets constructed from imidazole and (+)-**1**·Im and (−)-**2**·Im. Finally, as expected the fingerprint plot for (+)-**1**/(−)-**2**·BPDO exhibits unique features as compared to the other plots presented in this study. Fig. 5 shows distinct patterns for Cl/Br···H and π···π interactions.

4 Conclusions

Our results suggest that combining succinic acids (−)-**1** and (+)-**2** is generally destabilizing compared to forming crystals of the starting optically active components. This observation is consistent with Centnerszwer's 1899 melting-point data that reports a nearly 20 degree depression in melting-points for the racemate of **1** and quasiracemic phases. To circumvent this supramolecular difficulty, the inclusion of additional molecules capable of complementing the hydrogen-bond ability of succinic acids **1** and **2** were pursued and utilized in the study. Both imidazole (Im) and 4,4′-bipyridyl-*N*,*N*′-dioxide (BPDO) served as ternary components that altered the crystal packing landscape of **1** and **2**. Combining imidazole with the quasiracemate, racemate, and enantiopure forms of **1** and **2** resulted in crystal structures identified by molecular layers formed from strong N^+–H···carboxylate and carboxyl···carboxylate interactions. In contrast to the enantiopure [(+)-**1**·Im and (−)-**2**·Im] and racemic [(±)-**1**·Im and (±)-**2**·Im] systems, neighboring molecular layers observed in quasiracemate (+)-**1**/(−)-**2**·Im are organized by approximate inversion symmetry. Assessment of the crystal packing efficiency for this series of molecular salts *via* crystal densities and packing coefficients (C_k) indicates imidazole effectively alters the crystal landscape of the system in favor of racemate and quasiracemate formation. A similar desymmetrized crystal environment was also observed for the crystal structure of (+)-**1**/(−)-**2**·BPDO where the components are organized *via* N^+–O^-···carboxyl contacts. This study underscores the importance of molecular shape to molecular recognition processes and the stabilizing effect of tailor-made coformer molecules for creating new crystalline phases of previously inaccessible crystals.

Acknowledgements

This work was supported by the National Science Foundation (DMR-1505717 and CHE-0722547) and Eastern Illinois University CFR (KAW) and URSCA (JMS) awards.

Notes and references

1 F. Bächle, I. Fleischer and A. Pfaltz, *Adv. Synth. Catal.*, 2015, **357**, 2247.
2 S. Piovesana, R. Samperi, A. Laganà and M. Bell, *Chem.–Eur. J.*, 2013, **19**, 11478.
3 Y. Lu, A. J. Bolokowicz, S. A. Reeb, J. D. Wiseman and K. A. Wheeler, *RSC Adv.*, 2014, **4**, 8125.
4 E. A.-H. Yeh, E. Kumli, K. Damodaran and D. P. Curran, *J. Am. Chem. Soc.*, 2013, **135**, 1577.
5 F. Cardona, D. Lalli, C. Faggi, A. Goti and A. Brandi, *J. Org. Chem.*, 2008, **73**, 1999.
6 N. A. Shaye, S. Chavda, E. Coulbeck, J. Eames and Y. Yohannes, *Tetrahedron: Asymmetry*, 2011, **22**, 439.
7 C. H. Gorbitz and P. Karen, *J. Phys. Chem. B*, 2015, **119**, 4975.
8 J. T. Cross, N. A. Rossi, M. Serafin and K. A. Wheeler, *CrystEngComm*, 2014, **16**, 7251.
9 F. T. Martins, R. S. Correa, A. A. Batista and J. Ellena, *CrystEngComm*, 2014, **16**, 7013.
10 J. Jacques, A. Collet and S. H. Wilen, *Enantiomers, Racemates and Resolutions*, Wiley-Interscience, New York, 1981.
11 B. Dalhus and C. H. Gorbitz, *Acta Crystallogr., Sect. B: Struct. Sci.*, 2000, **B56**, 715.
12 M. Hendi, P. Hooter, V. Lynch, R. E. Davis and K. A. Wheeler, *Cryst. Growth Des.*, 2004, **4**, 95.
13 Q. Zhang and D. P. Curran, *Chem.–Eur. J.*, 2005, **11**, 4866.
14 S. P. Kelley, L. Fábián and C. P. Brock, *Acta Crystallogr., Sect. B: Struct. Sci.*, 2011, **B67**, 79.
15 Z. Hayouka, N. C. Thomas, D. E. Mortenson, K. A. Satyshur, B. Weisblum, K. T. Forest and S. H. Gellman, *J. Am. Chem. Soc.*, 2015, **137**, 11884.
16 C. K. Wang, G. J. King, S. E. Northfield, P. G. Ojeda and D. J. Craik, *Angew. Chem., Int. Ed.*, 2014, **53**, 11236.
17 L. Pasteur, *Ann. Chim. Phys., Ser.*, 1853, **38**, 437.

18 M. Z. Centnerszwer, *J. Phys. Chem.*, 1899, **29**, 715.
19 J. Timmermans and M. Dumont, *Bull. Soc. Chim. Belg.*, 1931, **40**, 689.
20 A. Fredga, *Bull. Soc. Chim. Fr.*, 1973, **1**, 173.
21 A. Gavezzotti and L. L. Presti, *Cryst. Growth Des.*, 2015, **15**, 3792.
22 R. Centore, S. Fusco, F. Capone and M. Causà, *Cryst. Growth Des.*, 2016, **16**, 2260.
23 K. A. Wheeler, R. C. Grove, R. E. Davis and W. S. Kassel, *Angew. Chem., Int. Ed. Engl.*, 2008, **47**, 78.
24 M. E. Breen, S. L. Tameze, W. G. Dougherty, W. S. Kassel and K. A. Wheeler, *Cryst. Growth Des.*, 2008, **8**, 3483.
25 J. E. Robinson and M. A. Brimble, *Org. Biomol. Chem.*, 2007, **5**, 2572.
26 B. J. Naysmith and M. A. Brimble, *Org. Lett.*, 2013, **15**, 2006.
27 G. M. Sheldrick, *SADABS — Program for Area Detector Absorption Corrections*, University of Göttingen, Göttingen, Germany, 2013.
28 L. J. Barbour, *J. Supramol. Chem.*, 2001, **1**, 189.
29 G. M. Sheldrick, *Acta Crystallogr., Sect. A: Found. Crystallogr.*, 2008, **64**, 112.
30 H. D. Flack, *Acta Crystallogr.*, 1983, **39**, 876.
31 M. Hendi, M. R. E. Davis, V. Lynch and K. A. Wheeler, *Cryst. Eng.*, 2001, **4**, 11.
32 F. H. Allen, *Acta Crystallogr., Sect. B: Struct. Sci.*, 2002, **B58**, 380.
33 L. Kryger, S. E. Rasmussen and J. Danielsen, *Acta Chem. Scand.*, 1972, **26**, 2339.
34 J. F. Britten, H. E. Howard-Lock, D. Leblanc and C. J. L. Lock, *Acta Crystallogr., Sect. C: Cryst. Struct. Commun.*, 1993, **49**, 1222.
35 A search of the CSD (version 5.37) for organic carboxylic acid structures containing ≤20 atoms with only C, H and one X group (X = Cl or Br) resulted in 27 (Cl) and 22 (Br) entries with average crystal densities of 1.543 and 1.824 g mL^{-1}, respectively.
36 The packing coefficient is defined as the ratio of the volume of the molecules in the unit cell to the volume of the unit cell, $C_k = V_{mol}/V_{cell}$: A. I. Kitaigorodsky, *Molecular Crystals and Molecules*, Academic Press, New York, 1973.
37 Molecular volumes were calculated using CPK model functions in *Spartan10* (Wavefunction, Inc.). For the imidazolium succinate structures, the volumes of the 1, 2, and imidazolium components were determined by calculating V_{mol} for each molecular species and averaging over the family of crystal structures.
38 A. Wong, K. J. Pike, R. Jenkins, G. J. Clarkson, T. Anupold, A. P. Howes, D. H. G. Crout, A. Samoson, R. Dupree and M. E. Smith, *J. Phys. Chem. A*, 2006, **110**, 1824.
39 A. Fischer, *Acta Crystallogr., Sect. E: Struct. Rep. Online*, 2006, **62**, o4190.
40 M. B. J. Atkinson, S. V. S. Mariappan, D.-K. Bučar, J. Baltrusaitisa, T. Friščić, N. G. Sinada and L. R. MacGillivray, *Proc. Natl. Acad. Sci. U. S. A.*, 2011, **108**, 10974.
41 J. Wouters and L. Quéré, *Pharmaceuticals Salts and Co-crystals, RSC Drug Discovery Series No.16*, Royal Society of Chemistry, Cambridge, UK, 2012, vol. 330.
42 F. H. Allen, W. D. S. Motherwell, P. R. Raithby, G. P. Shields and R. Taylor, *New J. Chem.*, 1999, 25–34.
43 J. C. MacDonald, P. C. Dorrestein and M. M. Pilley, *Cryst. Growth Des.*, 2001, **1**, 29.
44 S. A. Reeb, M. C. Shields and K. A. Wheeler, *Acta Crystallogr., Sect. E: Struct. Rep. Online*, 2009, **65**, o1424.
45 Y. X. Zhi, J. Hu, J. Y. Chen and J.-Z. Chen, *Z. Kristallogr.–New Cryst. Struct.*, 2009, **224**, 489.
46 A. Briceno, D. Leal and G. D. de Delgado, *New J. Chem.*, 2015, **39**, 4965.
47 J. M. Xiao, *Acta Crystallogr., Sect. E: Struct. Rep. Online*, 2009, **65**, o1157.
48 O. Wallach, *Liebigs Ann. Chem.*, 1895, **286**, 90.
49 C. P. Brock, W. B. Schweizer and J. D. Dunitz, *J. Am. Chem. Soc.*, 1991, **113**, 9811.
50 B.-Q. Ma, S. Gao, H.-L. Sun and G.-X. Xu, *CrystEngComm*, 2001, **3**, 147.
51 F. L. Hirshfeld, *Theor. Chim. Acta*, 1977, **44**, 129.
52 M. A. Spackman and D. Jayatilaka, *CrystEngComm*, 2009, **11**, 19.
53 M. A. Spackman and J. J. McKinnon, *CrystEngComm*, 2002, **4**, 378.